Comparison of previous results of the PbP and sequential emission modelings with the recent experimental data of Göök et al.

Anabella Tudora , Bucharest, August 2018

The first and most important validation of a prompt emission model consists of the comparison of the multi-parametric matrices of different quantities (e.g. prompt neutron multiplicity ν(A,TKE), average center-of-mass energy of prompt neutrons <ε>(A,TKE), average prompt γ-ray energy Eγ(A,TKE), etc.) with the existing experimental data. This comparison *validates the prompt emission model itself* because the fragment distribution Y(A,TKE) is not involved.

The comparison of different single distributions of prompt emission quantities (e.g. ν(A), ν(TKE), <ε>(A), <ε>(TKE), Eγ(A) etc.) and of total average quantities (e.g. $<\nu_p>_{tot}$, $<E\gamma>_{tot}$, $<\varepsilon>_{tot}$, prompt neutron spectrum in the center-of-mass and laboratory frames, etc.) with the experimental data *validates the prompt emission model together with the Y(A,TKE) distribution* (on which the multi-parametric matrices of different quantities, as primary model results, are averaged).

The detailed comparison of the model results of multi-parametric matrices with existing experimental data for different quantities can be made by using the 2D representations of:
- the quantity as a function of TKE for a given fragment mass
- the quantity as a function of A for a given TKE value

The recent experimental data of the prompt neutron multiplicity ν(A,TKE) for ^{235}U(n,f) measured by Göök et al. [1] offer the possibility to validate the PbP and sequential emission models themselves.

These experimental data (as the result of measurements performed over the incident neutron energy range 0.26 eV – 45 keV) are compared with the previous results at thermal incident neutron energy provided by the PbP model [2] and the deterministic sequential emission modeling [3].

The same fragmentation range was used in both modelings [2, 3]. It was deterministically constructed by taking into account a large fragment mass range going from symmetric fission (A=118) up to a very asymmetric split (A_H=160, A_L=76). For each mass number A three charge numbers Z were taken as the nearest integer values above and below the most probable charge Zp(A) which is considered as Z_{UCD}(A) corrected with the charge polarization ΔZ(A). For each fragment pair a large TKE range is taken (in this case from 100 to 200 MeV with a step size of 5 MeV). The charge polarization ΔZ(A) and the rms(A) of the isobaric charge distribution (taken as a Gaussian function centered on Zp(A)) provided by the Zp model of Wahl [4] were used.

Note, the primary results of both modelings, PbP and sequential emission, are the prompt emission quantities as a function of fragment mass (A) and charge (Z) and as a function of total kinetic energy (TKE), generically labeled q(A,Z,TKE). In the sequential emission treatment different quantities of each emission sequence (indexed k) are calculated, i.e. q_k(A,Z,TKE). The multi-parametric matrix q(A,Z,TKE) is then obtained by averaging q_k(A,Z,TKE) over the number of sequences corresponding to the initial fragment A, Z at each TKE value.

For the comparison with experimental multi-parametric data of different prompt emission quantities, which are measured as a function of A and TKE, the matrices q(A,Z,TKE), provided by the PbP and sequential emission modelings as primary results, are averaged over the isobaric charge distributions p(Z,A) (taken as narrow Gaussian functions centered on the most probable charge Zp(A)).

Fig.1 shows the ν(A,TKE) data of Göök et al. [1] in the representation of prompt neutron multiplicity as a function of TKE for a given fragment mass number (open black squares for A_L, full gray circles for A_H and full black diamonds for the fragment mass pair) in comparison with the PbP and sequential emission model results (green, blue and red lines for A_L, A_H and fragment mass pair, respectively). The parts a)-c) of the figure include the comparison with the PbP results and the part d) the comparison with the sequential emission results. The fragment mass numbers are indicated in each frame.

The experimental ν(A,TKE) data in the representation of prompt neutron multiplicity as a function of mass for a given TKE value (full black squares) are compared with the PbP result (red circles) in **Figs.2** and **3** and with the sequential emission result (blue stars) in **Fig.4**.

The excellent description of the ν(A,TKE) data of Göök et al. [1] by the PbP model result previously reported in Ref.[2] is easily seen in **Figs.1a-c, 2** and **3**.

It can be also observed that for fragmentations near symmetry (i.e. A_H less than 133, A_L great than 103) the experimental data at lower TKE values are spread, with large error bars and in the case of prompt neutron multiplicity as a function of TKE (Fig.1) they deviate from the linear trend due to the low yield and the contamination of background events.

In the case of sequential emission results previously reported in Ref.[3], see **Fig.1d** and **Fig.4**, the agreement with the experimental data of Göök is also good but not so remarkable as in the case of PbP results. The explication consists of the limited number of initial fragments taken into account in the treatment of sequential emission. This fact is visible especially for initial fragmentations with A_H around 130 for which the heavy fragments (often magic or double magic, i.e. Z=50, N=82) frequently cannot emit prompt neutrons, leading to very low values of the prompt neutron multiplicity corresponding to the heavy fragment mass number. The staggering exhibited by the sequential emission results given in Fig.1d is also due to the limited number of initial fragmentations taken into account in the deterministic construction of the initial fragmentation range. In the case of the PbP model, even if the fragmentation range is the same, this situation is avoided by the global treatment of the sequential emission using the residual temperature distribution P(T) which covers the entire process of successive neutron emission corresponding to each initial fragment.

Consequently the ν(A,TKE) results for $^{235}U(n_{th},f)$ provided by the PbP and sequential emission modelings reported in Refs.[2, 3] are confirmed by the subsequent measurements of Göök et al. [1]. This fact can be considered as a very valuable validation of both modelings.

Single distributions of different prompt emission quantities (e.g. ν(A), ν(TKE), <ε>(A) etc.) as well as prompt fission neutron spectra (PFNS) in the center-of-mass and laboratory frames and other total average quantities (e.g. $<\nu_p>_{tot}$, $<\varepsilon>_{tot}$ etc.) can be obtained by averaging the corresponding multi-parametric matrices provided by the PbP and sequential emission modelings over two experimental Y(A,TKE) distributions, i.e. of Göök et al. [1] and of Al-Adili et al. [5].

Note, the double distribution Y(A,TKE) of Al-Adili et al. was reconstructed from the single distribution data, i.e. Y(A), TKE(A) and $\sigma_{TKE}(A)$. It was already used to obtain the single distributions of different prompt emission quantities reported in Refs.[2, 3]. The recent distribution of Göök et al. is provided as Y(TKE) data at each A_H [1].

The Y(A,TKE) distributions of Göök and Al-Adili are compared in **Fig.5** via the projections Y(A) (left part), Y(TKE) (upper right part) and the TKE(A) data (lower right part). The data of Al-Adili et al. [5] are plotted with black squares and those of Göök et al. with red circles.

Non-negligible differences between the Y(A) data of Göök and Al-Adili are visible especially near symmetry and around the most probable fragmentation, too. A slight shift of the

Y(TKE) data of Göök compared to Al-Adili is observed. Large differences between the TKE(A) data of Göök and Al-Adili are visible at A_H from symmetric fragmentation up to 130. Differences between the TKE(A) data are also observed at very asymmetric fragmentations, i.e. A_H above 155.

The differences between the fragment distributions of Göök and Al-Adili should be due to the better analysis procedure sued by Göök et al. compared to the previous experiment of Al-Adili et al. when the priority was the investigation of ^{234}U(n,f), the ^{235}U(n_{th},f) reaction being measured only as a reference (not looking in detail to the distribution especially in the symmetry region).

Obviously these differences in fragment distributions induce differences between the single distributions of different prompt emission quantities obtained by averaging the same multi-parametric matrix over two Y(A,TKE) distributions.

The prompt neutron single distributions ν(A) and ν(TKE) are given in **Fig.6**: the experimental data of Göök et al. with full black diamonds and symbols with a cross inside), the results obtained by averaging the PbP matrix of ν(A,TKE) over the Y(A,TKE) distribution of Al-Adili (already reported in Ref.[2]) with red symbols and over the distribution of Göök with blue symbols. Other data sets of ν(A) taken from EXFOR are given in the upper part with different full gray and open black symbols.

As it can be seen in the upper part of **Fig.6**, pronounced differences between the ν(A) results based on the Y(A,TKE) distributions of Göök and Al-Adili are observed near symmetry. They are due to the differences in Y(A) near symmetry, i.e. the higher Y(A) of Al-Adili compared to Göök is reflected in higher ν(A) near symmetry.

In the case of ν(TKE) (lower part of Fig.6) the PbP results obtained by averaging over the two Y(A,TKE) distributions are very close to each other. The differences can be considered as insignificant reflecting the much lower differences in the Y(TKE) projections compared to the Y(A) projections. Note, the ν(TKE) result corresponding to the Y(A,TKE) distribution of Göök (blue symbols) starts from TKE of 141 MeV because the Y(A,TKE) data of Göök also start at this TKE value, while the Y(A,TKE) data of Al-Adili cover a larger TKE range (staring from 100 MeV).

In **Fig.7** the new ν(TKE) data of Göök et al. (black squares) are compared with the previously reported results of all prompt emission codes as following:

- two ν(TKE) results of PbP: one obtained by averaging the PbP matrix of ν(A,TKE) over the Y(A,TKE) of Al-Adili et al. which was reported in Refs.[2] and [6] (red circles connected with a solid line) and another obtained by averaging the same ν(A,TKE) matrix over the Y(A,TKE) of Göök (blue circles connected with a solid line).
- the ν(TKE) results of the codes FIFRELIN (orange line), CGMF (violet line) and FREYA (dark yellow line) reported in Ref.[6].
- the ν(TKE) result of the GEF code [7] performed in 2017 with the code version of 2015 (open green circles connected with a thin line).

As it can be seen the ν(TKE) results of PbP and GEF describe very well the experimental data of Göök et al. (this good agreement is better seen in the lower part of Fig.7 where only these results are given) while the results of FIFRELIN, CGMF and FREYA visibly deviate from the data.

Another valuable comparison regards the prompt fission neutron spectrum in the center-of-mass frame Φ(ε), because the experimental data of this quantity are almost inexistent. Fortunately the recent experimental Φ(ε) data Göök et al. [1] offer this possibility.

Fig.8, shows the PbP result of Φ(ε) [2] in comparison with the data Göök et al. (re-normalized to the calculated spectrum) For a better visualization, the figure includes two frames focusing the low and high energy parts of the spectrum. As it can be seen the PbP result of Φ(ε)

describes very well the experimental data over the entire prompt neutron energy range. Only at high energies, above 7 MeV, a slight overestimation of a great part of the spread experimental data with large error bars is observed.

As it can be seen in **Fig.9,** the PbP results of the average spectra in the center-of-mass frame corresponding to the light and heavy fragment groups $\Phi_{L,H}(\varepsilon)$ are in an excellent agreement with the data of Göök for selected fragment mass ranges around the most probable fragmentation. Again for a better visualization the high and low energy parts of the spectra are focused in separate frames.

It is interesting to mention that in the case of center-of-mass spectra corresponding to the light and heavy fragment groups the very good agreement with the experimental data is accomplished over the entire energy range, including the high energies above 7 MeV (where the total spectrum, corresponding to all fragments, exhibits a very slow underestimation of a great part of data).

The first order momenta of the center-of mass spectrum for each fragment mass $\Phi(\varepsilon,A)$ are plotted in **Fig.10** as following:
- the $<\varepsilon>(A)$ result reported in Ref.[2] (obtained by averaging the PbP matrix of $<\varepsilon>(A,TKE)$ over the Y(A,TKE) distribution of Al-Adili [5]) with red circles
- $<\varepsilon>(A)$ obtained by averaging the same PbP matrix of $<\varepsilon>(A,TKE)$ over the Y(A,TKE) data of Göök et al. [1] with blue diamonds
- the recent $<\varepsilon>(A)$ data of Göök et al. [1] with black squares.

The PbP results of $<\varepsilon>(A)$ based on the distributions of Al-Adili and Göök differ from each other only near symmetry as a consequence of the non-negligible differences between the Y(A) data of Al-Adili and Göök in this A region. In the fragment mass region of asymmetric fission the PbP results describe well the experimental $<\varepsilon>(A)$ data of Göök et al.

The total average values of the center-of-mass energy of prompt neutrons are indicated in the figure, too. In the case of experimental data, both $<\varepsilon>_{tot}$ values (obtained by averaging the $<\varepsilon>(A)$ data of Göök over the Y(A) distributions of Al-Adili and Göök) are given. The PbP results of $<\varepsilon>_{tot}$ differ from the experimental $<\varepsilon>_{tot}$ data with 0.2% (in the case of the fragment distribution of Al-Adili) and 1.2% (in the case of the fragment distribution of Göök).

Fig.11 shows the prompt fission neutron spectrum in the laboratory frame in the usual representation as ratio to a Maxwellian spectrum with TM = 1.35 MeV, the PbP result of Ref.[2] is plotted in comparison with the experimental data of Kornilov and Hambsch (black diamonds), of Vorobiev et al. (gray squares) and the new data of Göök et al. [1] (green circles). All experimental data sets are re-normalized to the calculated spectrum. Again for a better visualization the high and low energy parts of the spectrum are focused in separate frames.

As it can be seen the PbP result describes well all data sets. Considering the entire energy range of the spectrum, the best agreement is obtained with the data of Kornilov and Hambsch (χ^2 = 0.739), followed by the data of Göök (χ^2 = 0.947). It can be seen that they are very well described by the PbP spectrum up to about 8 MeV, above this energy the Göök data being lower than the other data sets and the calculated spectrum. It can be also observed that the PFNS data of Göök et al. [1] are close to the data of Kornilov and Hambsch up to about 7 MeV, exhibiting the same shape.

In **Fig.12** the new PFNS data of Göök et al. [1] (green circles) are also compared with the result of the Los Alamos (LA) model with non-equal Tm (maximum temperature of the residual temperature distribution) using the two sets of average model parameters which were proposed by Madland and Kahler [8] in order to describe separately the data sets of Kornilov and Hambsch (upper part of Fig.12) and of Vorobyev et al. (lower part).

As an observation, the differences in shape between the data of Göök and Vorobiev as well as the similar shapes exhibited by the data of Kornilov et al. and Göök et al. are better visible in Fig.12, being compared in separate frames.

It is well known that the spectrum shape is very sensitive to the compound nucleus cross-section of the inverse process of neutron evaporation from fragments $\sigma_c(\varepsilon)$ especially in the case of the LA model which uses only one fragmentation. In this case only two $\sigma_c(\varepsilon)$ corresponding to the light and heavy fragment of the most-probable fragmentation being involved. This fact is demonstrated in Fig.12. It can be seen that the shape exhibited by the experimental data of Kornilov and Hambsch and of Göök et al. is almost the same and it is well described by the LA model calculation using $\sigma_c(\varepsilon)$ provided by optical model calculations with the phenomenological parameterization of Becchetti-Greenlees, while the shape exhibited by the data of Vorobiev is reproduced by a LA model calculation using the optical model parameterization of Koning-Delaroche for $\sigma_c(\varepsilon)$. To describe the Vorobiev data at low prompt neutron energies it was necessary to include the anisotropy (with a parameter value b = 0.10).

In the case of the PbP model, many $\sigma_c(\varepsilon)$ of all fragments of the fragmentation range (exhibiting different shapes) are involved. In this case the total spectrum shape is influenced not only by the $\sigma_c(\varepsilon)$ of all fragments but also by the other parameters of fragments. Moreover the PbP spectrum of Fig.11 describes well the data at low energy without to consider the anisotropy.

References:

[1] A.Göök, *private communications* in June and July **2018.** A.Göök, F.-J.Hambsch, S.Oberstedt, M.Vidaly, "Prompt neutrons in correlation with fission fragments from 235U(n,f)", accepted for publication in *Phys.Rev.C* on **23 July 2018**.

[2] A.Tudora, F.-J.Hambsch, *Eur.Phys.J. A,* **53**(8) **(2017)** 159

[3] A.Tudora, F.-J.Hambsch, V.Tobosaru, *Eur.Phys.J. A*, **54**(5), **(2018)**, 87

[4] A.C.Wahl, *Atomic Data and Nuclear Data Tables* **39 (1988)** 1-156

[5] A.Al-Adili, F.-J.Hambsch, S.Pomp, S.Oberstedt, *Phys.Rev.C* **93**, **(2016)** 034603

[6] R. Capote, Chen Y.J., F.-J. Hambsch, N.V. Kornilov, J.P. Lestone, O. Litaize, B. Morillon, D. Neudecker, S. Oberstedt, T. Ohsawa, N. Otuka, V.G. Pronyaev, A. Saxena, O. Serot, O.A. Shcherbakov, Shu N.C., D.L. Smith, P. Talou, A. Trkov, A.C. Tudora, R. Vogt, S. Vorobyev, *Nucl.Data Sheets* **131 (2016)** 1-131.

[7] K-H.Schmidt, B.Jurado, C.Amoureux, C.Schmitt, *Nucl.Data Sheets* **131 (2016)** 107-221.

[8] D.G.Madland and A.C.Kahler, *Nucl.Phys.A* **957 (2017)** 289-311.

FIGURES

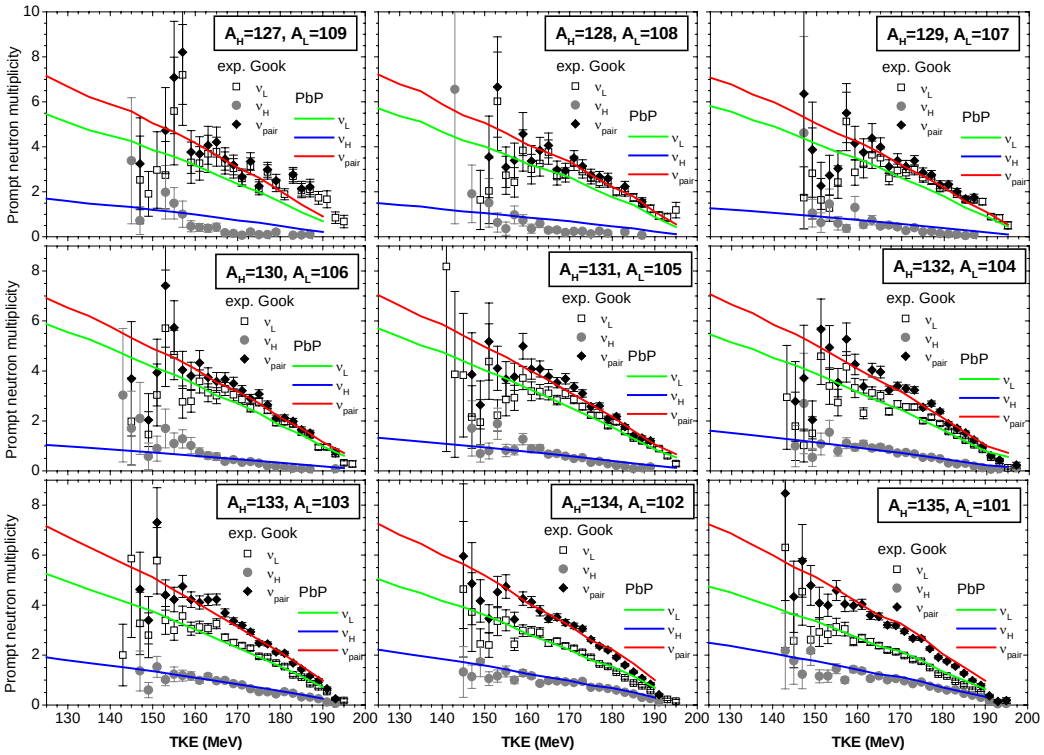
A_H=127, A_L=109
A_H=128, A_L=108
A_H=129, A_L=107
A_H=130, A_L=106
A_H=131, A_L=105
A_H=132, A_L=104
A_H=133, A_L=103
A_H=134, A_L=102
A_H=135, A_L=101
exp. Gook
PbP
Prompt neutron multiplicity
TKE (MeV)

a)

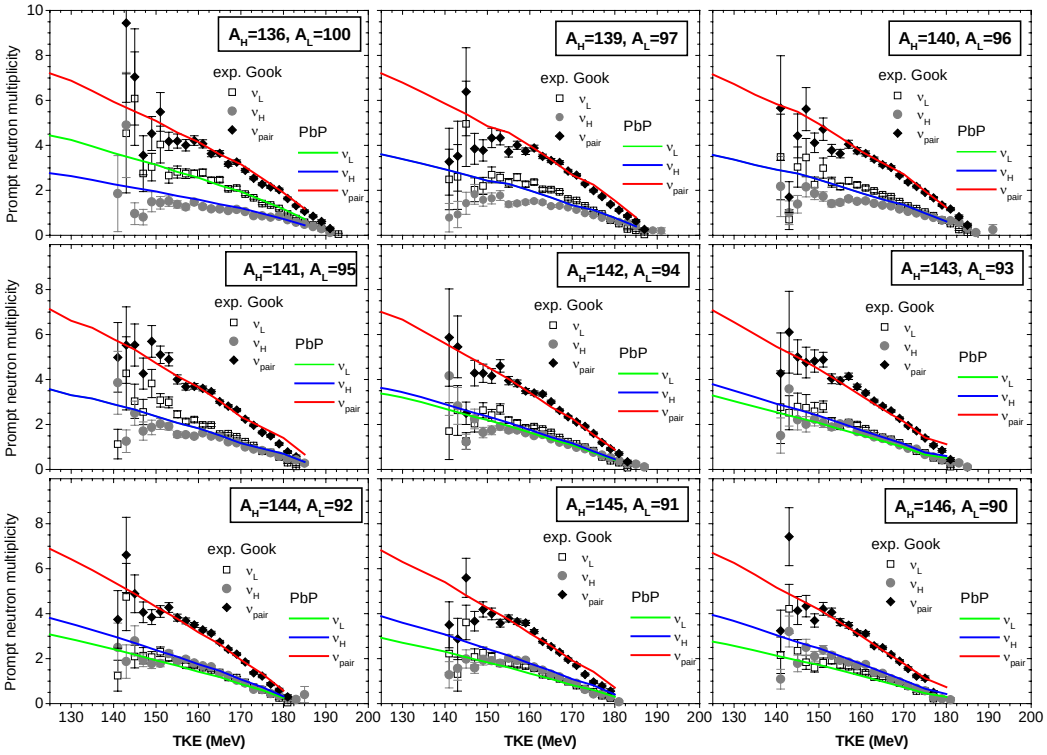
A_H=136, A_L=100
A_H=139, A_L=97
A_H=140, A_L=96
A_H=141, A_L=95
A_H=142, A_L=94
A_H=143, A_L=93
A_H=144, A_L=92
A_H=145, A_L=91
A_H=146, A_L=90
exp. Gook
PbP
Prompt neutron multiplicity
TKE (MeV)

b)

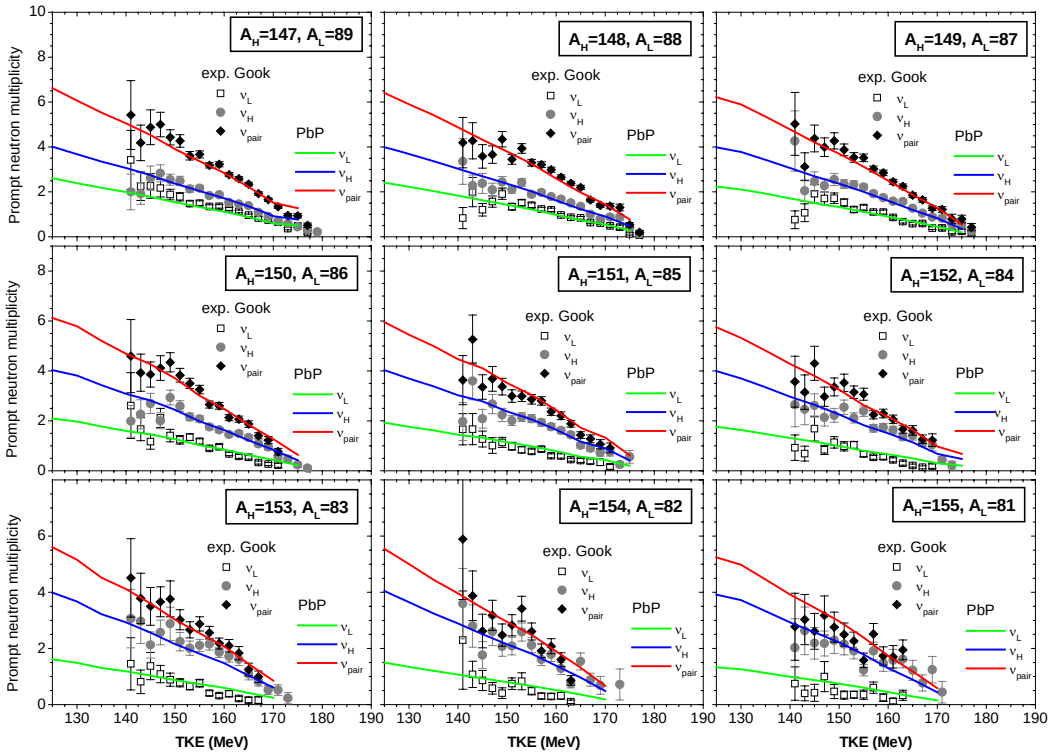

c)

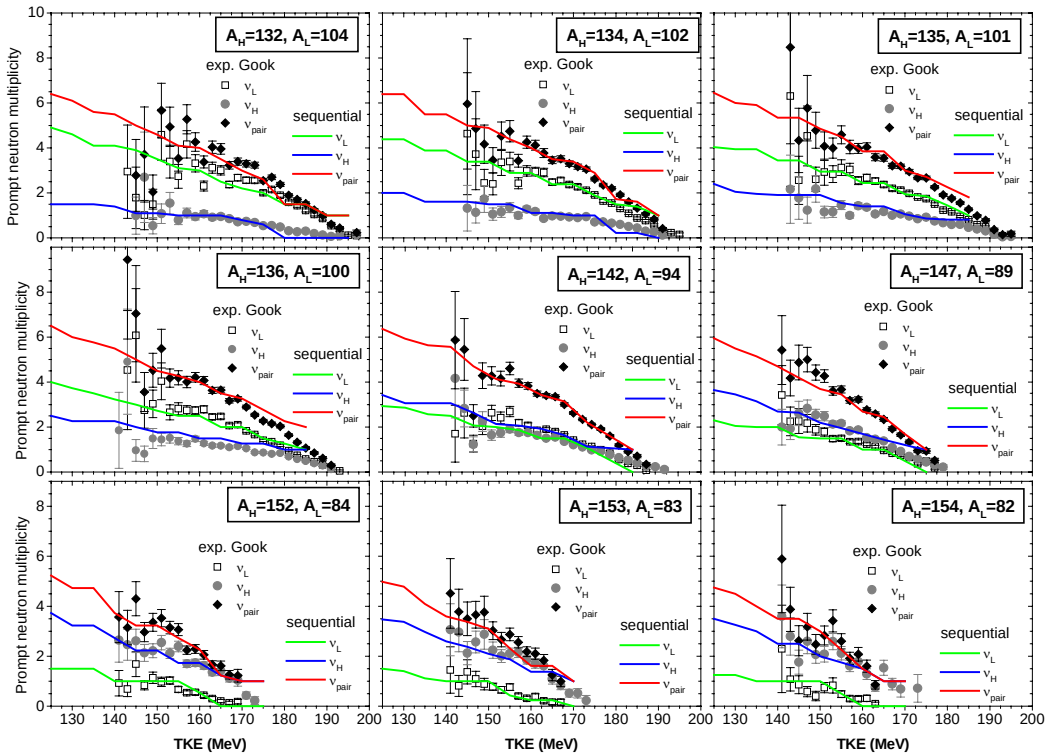

d)

Fig.1: Comparison of the ν(A,TKE) results of PbP (a-c) and sequential emission (d) with the data of Göök et al. in the representation of the prompt neutron multiplicity of the light and heavy fragments and of the fragment mass pair as a function of TKE for given fragment masses indicated in each frame.

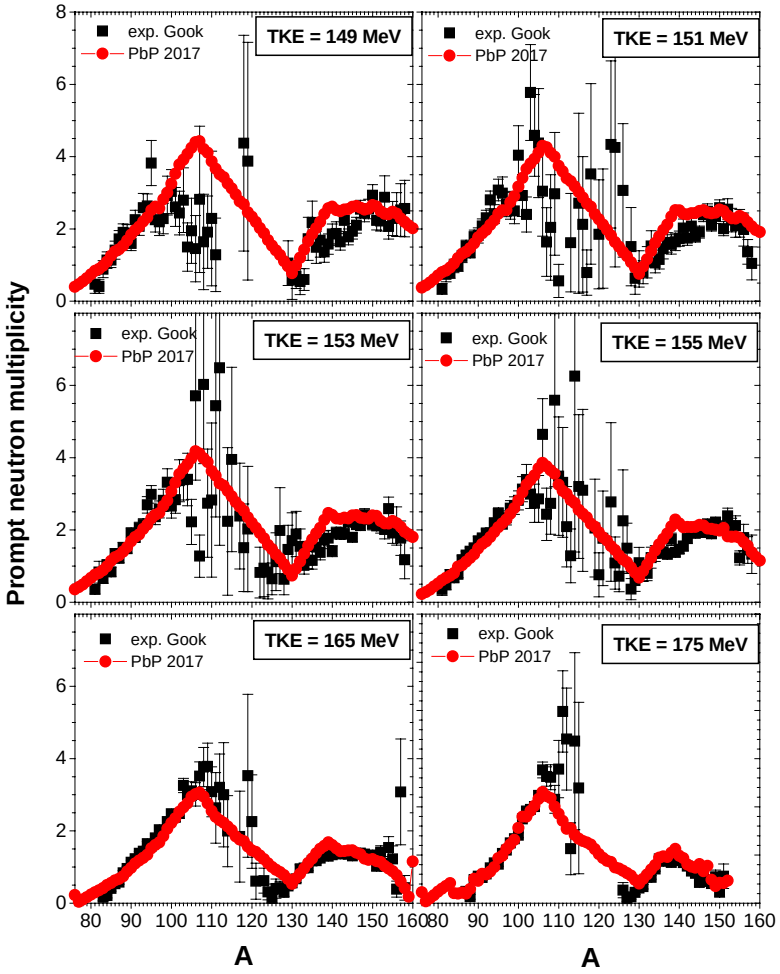

Fig.2: Comparison of the ν(A,TKE) matrix of PbP (red circles) with the experimental data of Göök et al. (black squares) in the representation of the prompt neutron multiplicity as a function of A at a given TKE value (indicated in each frame).

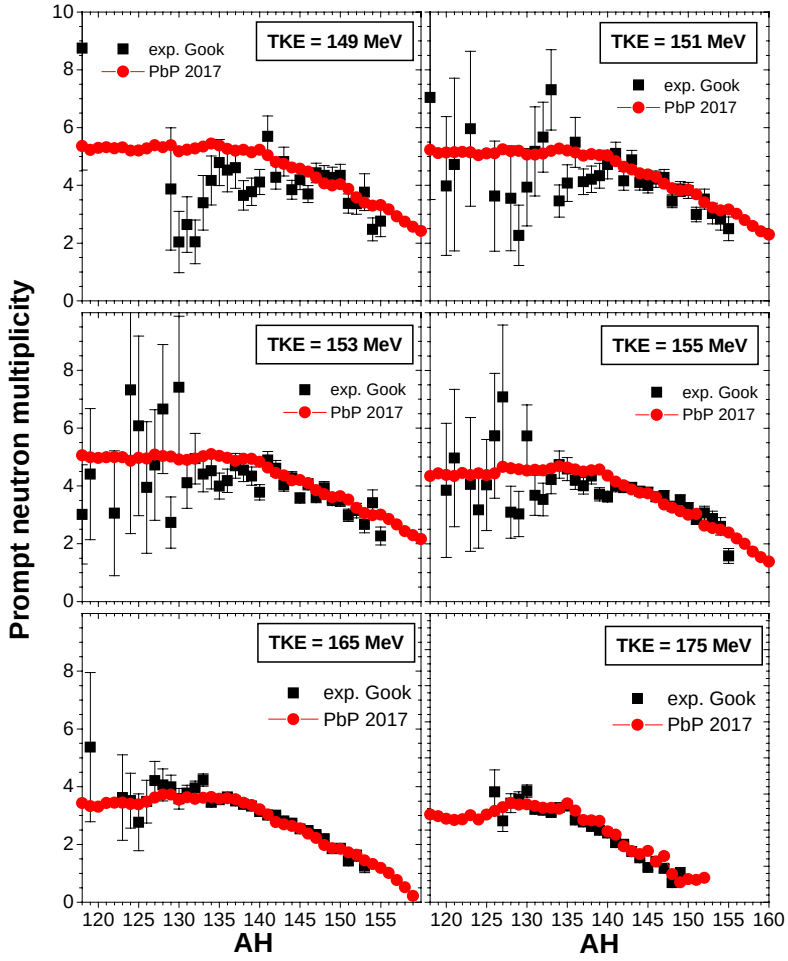

Fig.3: Comparison of the ν(A,TKE) matrix of PbP (red circles) with the experimental data of Göök et al. (black squares) in the representation of the prompt neutron multiplicity of fragment pair as a function of A_H at a given TKE value (indicated in each frame).

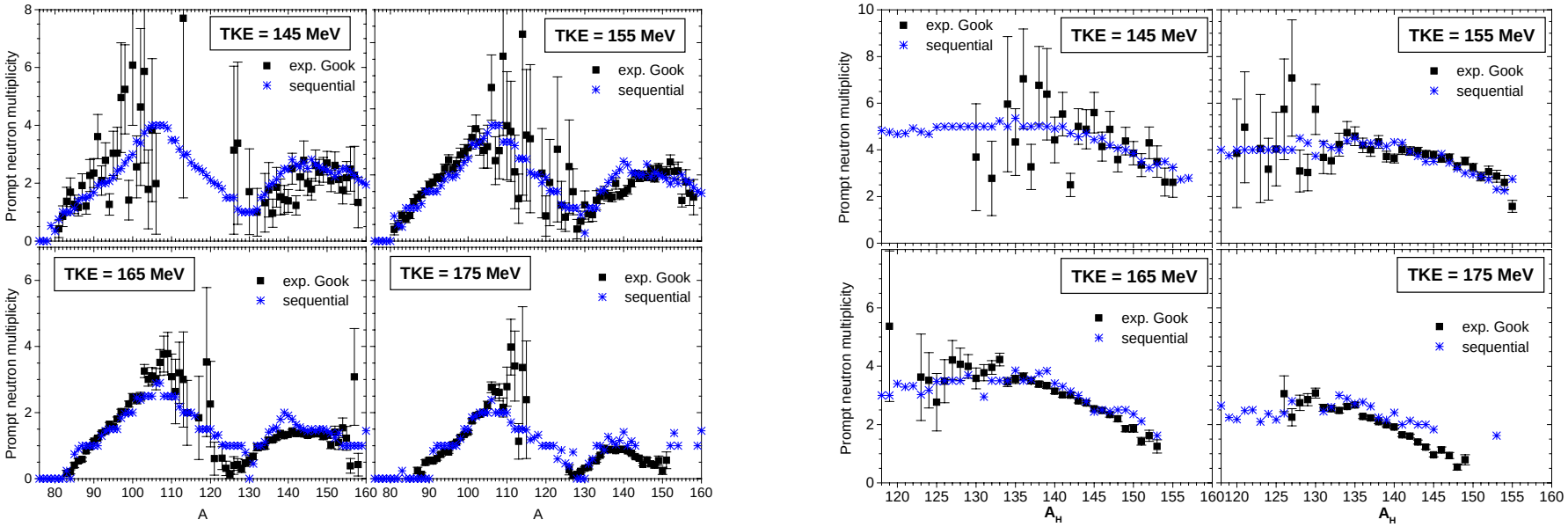

Fig.4: Comparison of the ν(A,TKE) matrix resulting from the sequential emission treatment (blue stars) with the experimental data of Göök et al. (black squares) in the representation of the prompt neutron multiplicity as a function of A (left part) and the prompt neutron multiplicity of fragment pair as a function of A_H (right part) at a given TKE value (indicated in each frame).

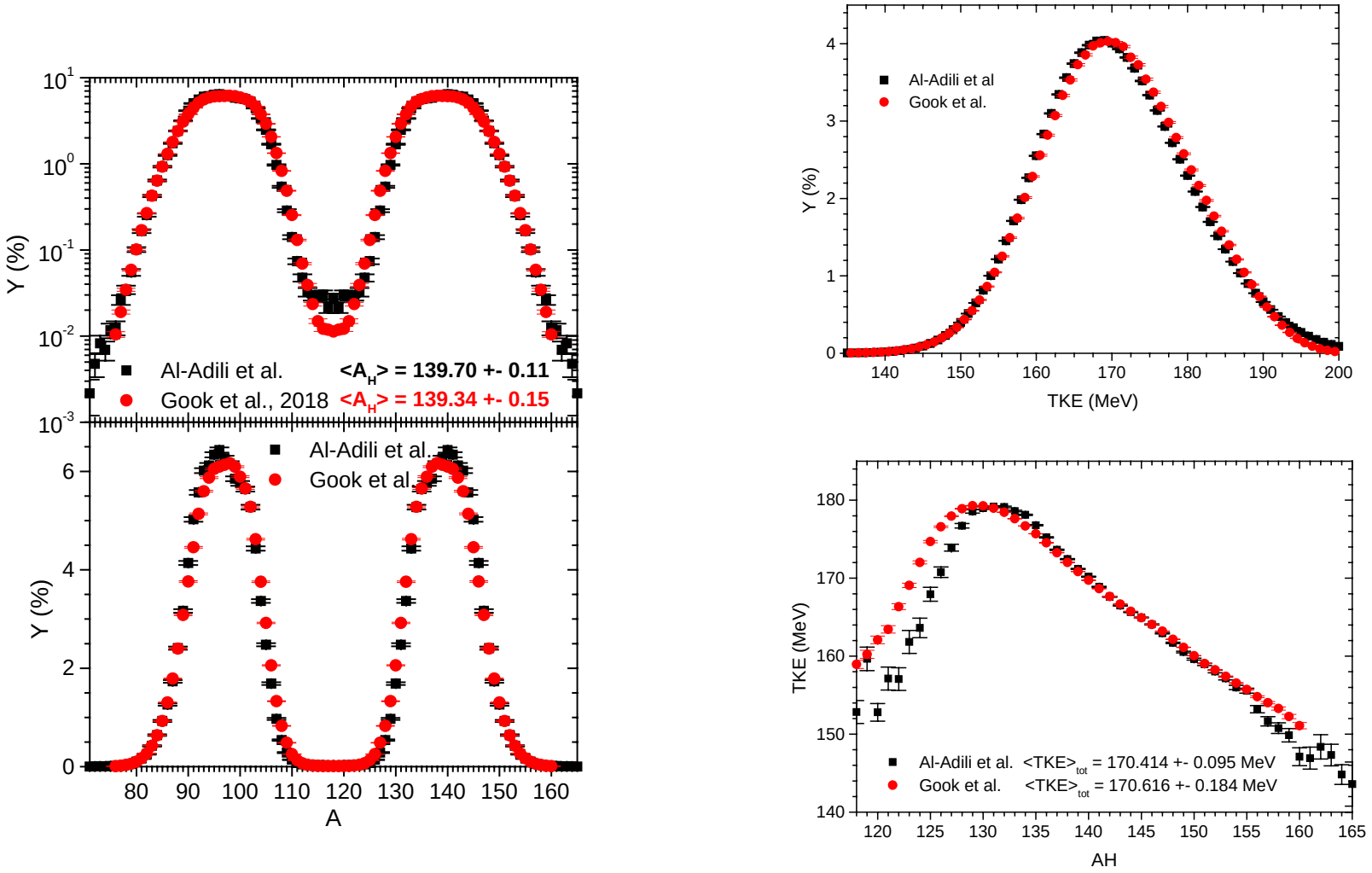

Fig.5: Experimental single distributions Y(A) (left part), Y(TKE) (right upper part) and TKE(A) (right lower part). The data of Al-Adili et al. are plotted with black squares and the data of Göök et al. with red circles.

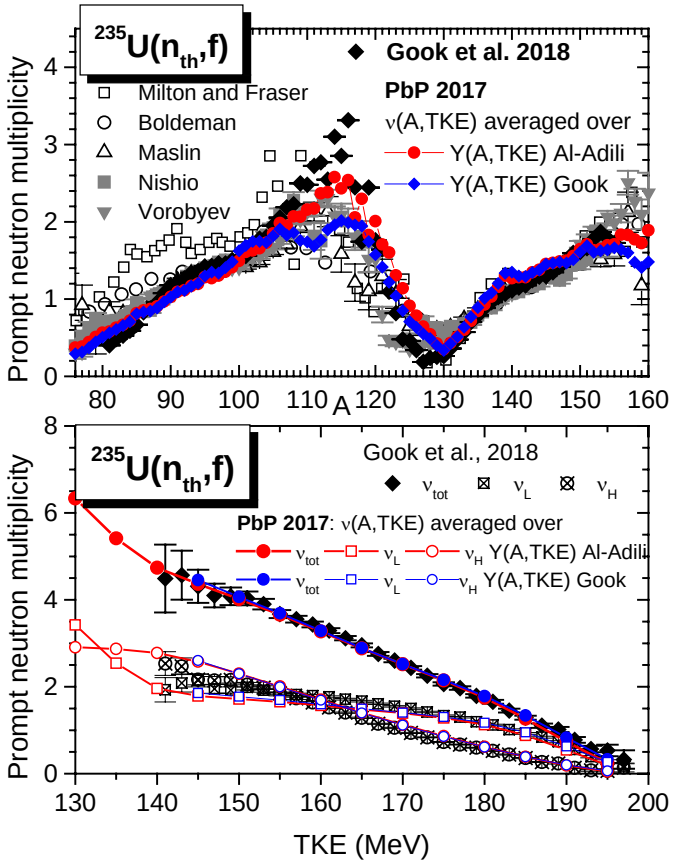

Fig.6: Average ν(A) (upper part) and ν(TKE) (lower part) obtained by averaging the ν(A,TKE) result of PbP over the Y(A,TKE) data of Al-Adili et al. (red symbols) and of Göök et al. (blue symbols) in comparison with the recent prompt neutron multiplicity data of Göök et al. (full black symbols and symbols with a cross inside). Other ν(A) data sets taken from EXFOR are also given in the upper part (with different full gray and open black symbols).

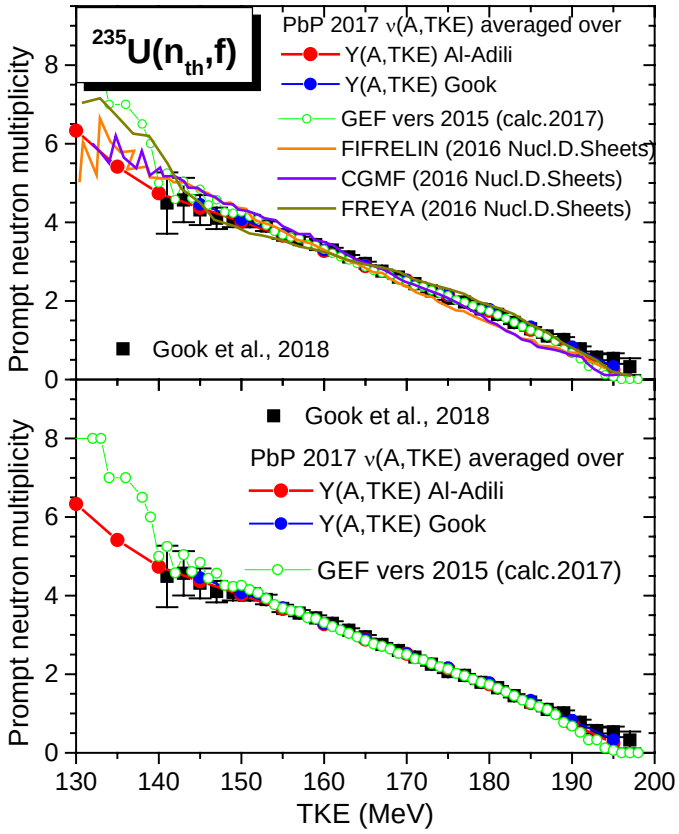

Fig.7: The ν(TKE) results of the prompt emission codes: PbP (full red and blue circles), GEF version 2015 (open green circles), FIFRELIN (orange line), CGMF (violet line) and FREYA (dark yellow line) in comparison with the data of Göök et al. (full black squares) The very good description of experimental ν(TKE) data by the PbP and GEF results is better seen in the lower part where only these results are plotted.

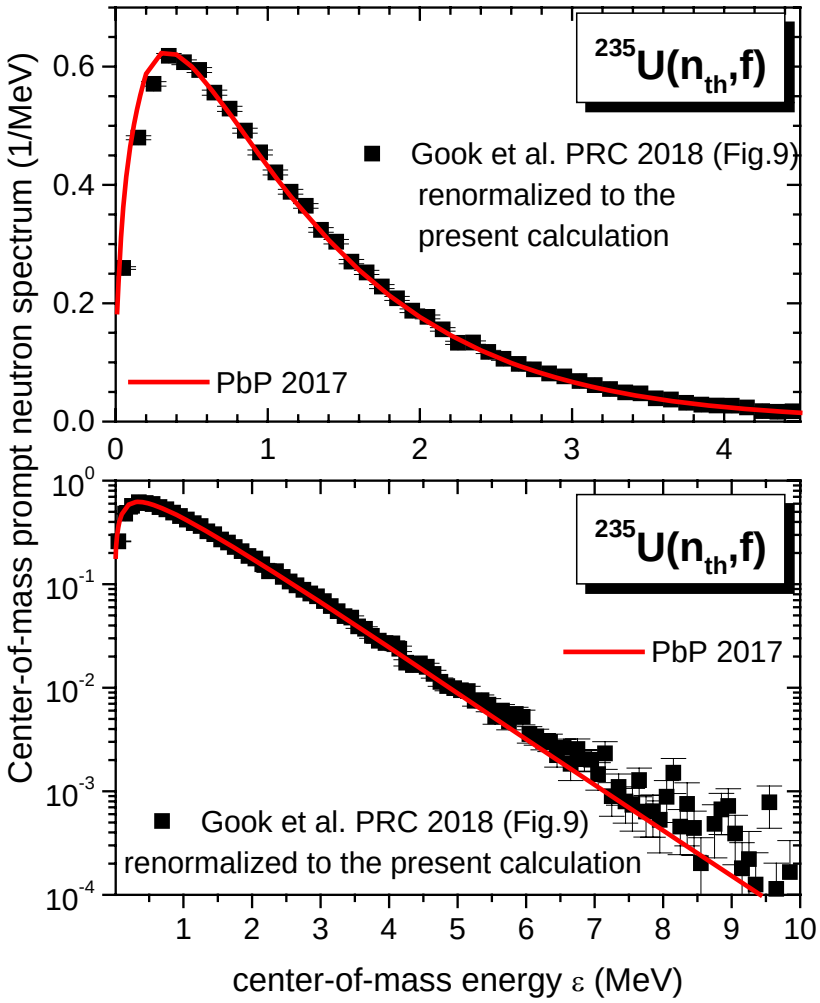

Fig.8: Prompt neutron spectrum in the center-of-mass frame: the recent data of Göök et al from Fig.9 of Ref.[1] (black symbols) in comparison with the previous PbP result of Ref.[2] (red line). The experimental data were re-normalized to the calculated spectrum.

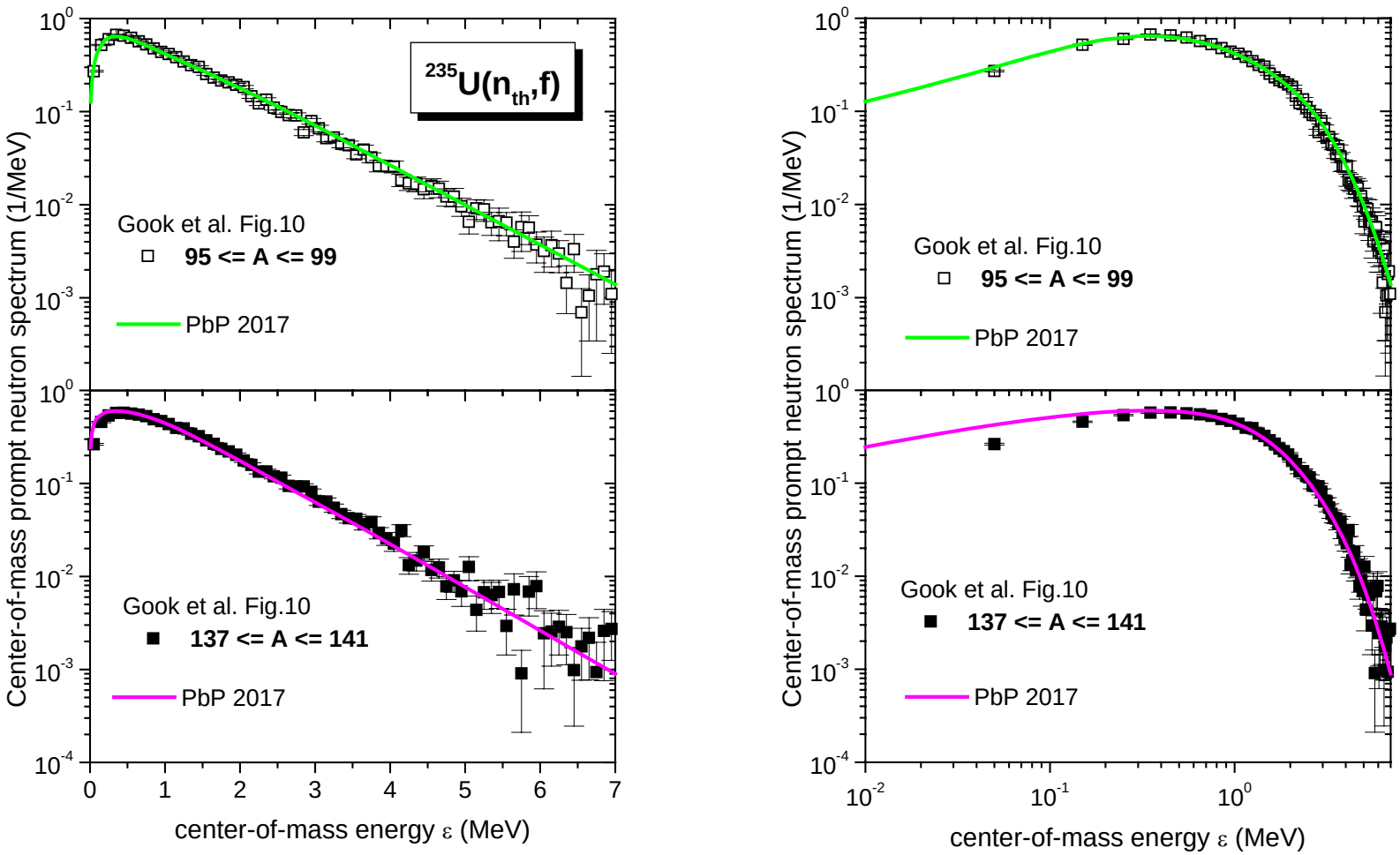

Fig.9: The experimental prompt neutron spectrum in the center-of-mass frame for selected fragment mass ranges around the most probable fragmentation from Fig.10 of Göök et al. [1] (light fragments in the upper part and heavy fragments in the lower part). The PbP results represent the spectrum obtained by averaging over the light and heavy fragment groups, respectively. The high energy part of the spectrum is focused in the left part of the figure and the low energy part of the spectrum in the right part.

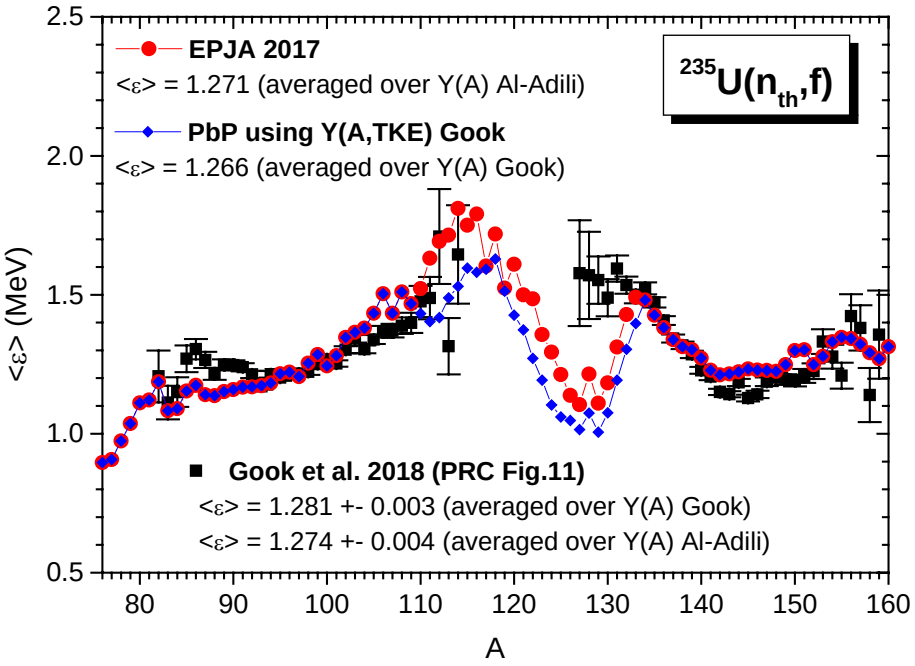

Fig.10: Experimental <ε>(A) data from Fig.11 of Göök et al. [1] (black squares) in comparison with the previous PbP result from Ref.[2] (red circles) and the result obtained by averaging the same <ε>(A,TKE) matrix of Ref.[2] over the Y(A,TKE) distribution of Göök (blue diamonds). The total average values obtained by averaging the experimental and calculated <ε>(A) over the Y(A) distributions of Al-Adili et al. and of Göök et al. are also indicated in the figure.

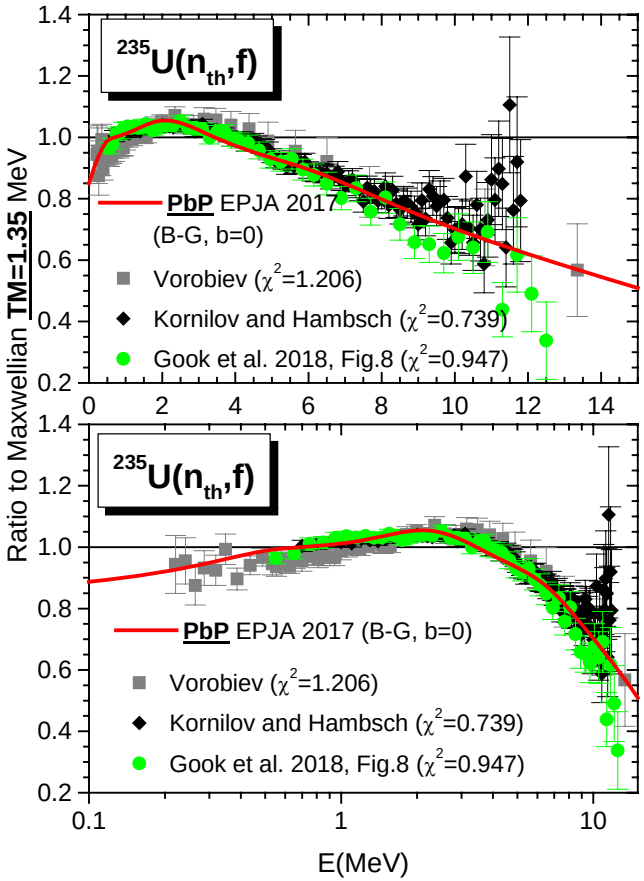

Fig.11: Comparison of the PFNS data of Göök et al. (green circles without error bars) with the previous PbP result of 2017 [2] (red line) and the experimental data sets of Vorobiev (gray squares) and of Kornilov and Hambsch (black diamonds). All experimental data sets are re-normalized to the calculated PFNS. The high and low energy parts of the spectrum are focused in separate frames.

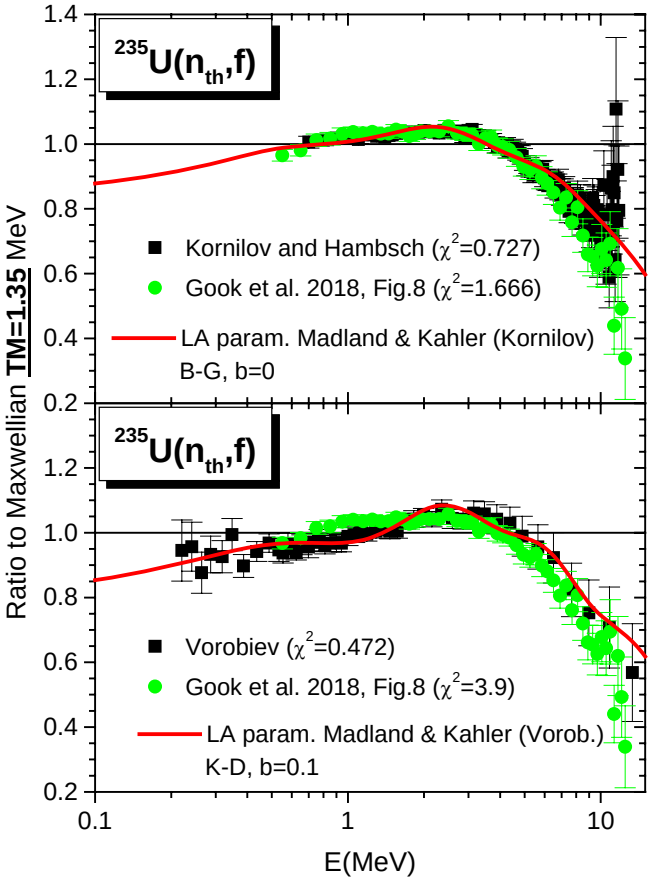

Fig.12: Comparison of the PFNS data of Göök et al. (green circles without error bars) with the previous results of the Los Alamos model with non-equal Tm (red lines) using the two sets of parameters reported by Madland and Kahler [8], i.e. the parameters leading to a good description of the data of Kornilov and Hambsch (upper part) and of the data of Vorobyev (lower part). The experimental data plotted in each frame were re-normalized to the calculated spectrum given in the respective frame.